Preliminary assessment of increased main engine load as a consequence of added wave resistance in the light of minimum propulsion po

Holt, Philip; Nielsen, Ulrik D.

Published in:
Applied Ocean Research

Link to article, DOI:
10.1016/j.apor.2021.102543

Publication date:
2021

Document Version
Peer reviewed version

PostPrint

Preliminary assessment of increased main engine load as a consequence of added wave resistance in the light of minimum propulsion power

Philip Holt[a], Ulrik D. Nielsen[b,c]

[a] *MAN Energy Solutions,* Copenhagen, Denmark
[b] *DTU Mechanical Engineering, Technical University of Denmark,* Kgs. Lyngby, Denmark
[c] *Centre for Autonomous Marine Operations and Systems, NTNU AMOS,* Trondheim, Norway

Abstract

This paper addresses the connection between added wave resistance and required propulsion power of ships, having focus on the early stage of new ship designs, notably tankers and bulk carriers. The paper investigates how mean added wave resistance affects the required torque of a fixed pitch propeller and thus also the operational conditions of a directly coupled main engine. The interest of the study has its background in the assessment of minimum propulsion power, and the study considers the prescriptive guidelines of the IMO as basis. Specifically, the study focuses on an assessment of the minimum forward speed attainable under consideration of the propeller light running margin and static load limits of engines in the early phase of new ship designs, where details of hull geometry are not available. The study considers three semi-empirical methods for predicting mean added wave resistance. All methods are known to be applied in the industry, emphasising that only methods relying solely on main particulars, together with information about sea state and advance speed, are of interest. The paper contains a case study used to illustrate the importance of the added wave resistance prediction with respect to the loading of the main engine. It is shown that, despite small absolute differences, the consequence in relation to the loading of the propeller and hereby the directly coupled main engine can be relatively large. Furthermore, the study illustrates that the propeller light running margin of a fixed pitch propeller directly coupled to the main engine has crucial influence on the attainable speed during adverse weather conditions.

Keywords:

Minimum propulsion power, engine load diagram, propeller light running margin, added wave resistance, semi-empirical methods

Holt and Nielsen (2021) in Applied Ocean Research DOI: 10.1016/j.apor.2021.102543

1. Introduction

The International Maritime Organization has released interim guidelines [1] on minimum propulsion power (MPP) for bulk carriers and tankers equipped with fixed pitch (FP) propellers. The guidelines are results of the tendency to reduce the power of the main engine installed on new ships; noting that a reduction in power allows the ship to attain a better energy efficiency design index (EEDI) [2], without changing from traditional fuel. However, the reduced main engine power may lead to a lower forward speed in adverse weather resulting in an increased risk of loosing manoeuvrability during encounters of heavy weather: The resistance from wind and waves may increase the torque required by the FP propeller to such an extent that the operational point (torque vs. rpm) continuously falls outside of the static load diagram of the typical prime mover, i.e. a two-stroke low speed marine engine, ultimately resulting in a reduction of engine speed. In such conditions, the advance speed drops and, ultimately, the ship may be prevented from steering into the dominant wave direction or even maintain a forward speed sufficient for keeping its course.

The present study, in line with assessment level 2 of the IMO guidelines on MPP [1] as described in the following section, focuses on a utilisation of three methods for estimating mean added wave resistance in head seas in order to predict the forward speed attainable under consideration of the static load limits of a main engine directly coupled to a FP propeller. This sole evaluation of the attainable minimum forward speed represents a simplified assessment of the complex situation of manoeuvring in adverse weather conditions. By this simplified approach, no considerations are given to a ship's capability to steer into the dominant wave direction, nor to dynamic limits of the directly coupled main engine, effects of dynamic propeller ventilation, wake fraction fluctuations, etc. Such effects are not considered in the present study, as the focus lies on an early evaluation of a design's compliance with [1]; but it is noteworthy that all effects are important to consider later in the design spiral, when the exact hull design, propeller, and main engine are known, thus making manoeuvring simulations or wave tank tests possible.

The focus of this study is solely on FP propellers and the effects of added wave resistance towards the operational point of the directly coupled main engine; that is, the study does not consider controllable pitch (CP) propellers. Although a CP propeller in theory can load a directly coupled main engine at any point within the engine load diagram in any condition and provides advantages with respect to manoeuvrability, FP propellers - as a result of higher efficiency and

lower cost - dominate the segment of larger merchant vessels performing week- or month-long ocean crossings.

1.1. Minimum propulsion power

As indicated, the MPP guidelines [1] are in place to evaluate the design of new ships with respect to required main engine power.* Essentially, the guidelines distinguish between two assessment levels, where the ship should be considered to have sufficient power to maintain the manoeuvrability in adverse conditions if it fulfils one of these assessment levels. Assessment level 1 relates the requirement for MPP to the capacity of the ship in deadweight tonnage (DWT) through the simple expression: MPP = $a \times$DWT + b, with coefficients a and b defined by [1].

Assessment level 2 constitutes an evaluation of the torque reserve between the main engine load limits and the light (design) propeller curve, rather than an evaluation of maximum power installed. Thus, on the basis of the mean added resistance resulting from the prescribed sea state for, it is evaluated if the increase of required torque of the FP propeller can be maintained/ensured within the static load limits of the main engine. The simplified principle of the assessment is that, if the propulsion plant can provide the required torque to propel the ship with a certain advance speed in head waves and wind, the ship will also be able to keep course in waves and wind from any other direction. The minimum ship speed of advance in head waves and wind is thus selected depending on ship design, in such a way that the fulfilment of the ship speed of advance requirements means fulfilment of course-keeping requirements [1]. As a result, all resistance components (i.e., bare hull resistance in calm water, resistance due to appendages, aerodynamic resistance, and added resistance due to waves) must be determined when assessment of MPP is made in accordance with level 2.

In accordance with [1], the minimum forward speed required to ensure course keeping is in the range 4-9 knots, depending on the ratio between frontal and lateral wind area and relative rudder area. Based on a ship's length between perpendiculars L_{pp}, level 2 of the MPP-guidelines defines two 'limiting sea states' as adverse conditions, in which the minimum forward speed is to be kept.

*The guidelines are initially for EEDI Phase 0 and 1, but are expected to be extended to include Phase 2 and Phase 3, possibly in a modified form.

The criteria for the significant wave height H_s and mean wind speed V_{wind} are:

$$L_{pp} < 200 \text{ m: } H_s = 4.0 \text{ m and } V_{wind} = 15.7 \text{ m/s} \quad (1)$$

$$L_{pp} > 250 \text{ m: } H_s = 5.5 \text{ m and } V_{wind} = 19 \text{ m/s} \quad (2)$$

where values are to be linearly interpolated for $200 \leq L_{pp} \leq 250$ m. Furthermore, assessment level 2 requires that MPP is calculated for a range of wave spectra, by varying the peak wave periods from 7.0 s to 15.0 s. The intervals of significant wave heights and wind speeds to be considered imply that two categories of ships are especially challenged: Ships of just $L_{pp} = 250$ m, and smaller ships of 20,000 DWT where the EEDI-requirements are full in phase for tankers and bulk carriers [2]. These smaller ships are typically significantly shorter than $L_{pp} = 200$ m, and therefore they will experience the relatively most severe sea state.

As the MPP requirement set by assessment level 1 often returns values which hinder traditionally fueled ships in attaining compliance with EEDI Phase 2, an increase in designs that will have to be evaluated at assessment level 2 is expected. On a side note, it is assumed that traditional fuels continue to dominate the new-building market and concerns about MPP are thus believed to be relevant throughout the next decade(s).

As pointed out above, in assessment level 2, the capabilities of the specific propulsion plant are considered relative to the total resistance on the ship. At low to vanishing speed in a severe sea, the added wave resistance will often be the major resistance component, especially for smaller ships. The added wave resistance on a ship can be computed if the associated transfer functions are available; and the MPP-guidelines require that the transfer functions are derived from model tests as per ITTC procedures [3, 4]. However, since model-scale tests can only be performed late in the design stage, uncertainty regarding a ship's performance in adverse conditions will be large in the early design phases, where the detailed hull geometry is not available. This concern has been reflected by debates about making updated MPP-guidelines in which model-scale tests can be replaced by a simple and reliable numerical model for estimation of the added wave resistance, recognising that the variation of main particulars and characteristic coefficients within the population of bulk carriers and tankers is limited. One approach to this has been proposed to the MEPC [5] based on joint work between SHOPERA[†] and the Japan Society of Naval Architects and Ocean

[†]Energy Efficient Safe SHip OPERAtions, see more at http://shopera.org/

Engineers; however, the sea state in which the ship is to be able to maintain safe manoeuvering could not be agreed on. A description of the work by SHOPERA [5, 6] is given in Section 2.1.2.

1.2. Scope and novelty of study

This study considers three semi-empirical numerical methods for predicting added wave resistance on ships; emphasising that the methods - as a constraint - take just the ship's main particulars as input. This means that the methods are useful for early resistance prediction in the design phase of ships, where detailed hull lines will not be available. The methods, which will be presented in some detail in Subsection 2.1, are the STAwave-2 method, the SHOPERA equation, and the DTU Design Tool where the latter is a computational method developed at the Technical University of Denmark.

The paper presents a small sensitivity study, where the three methods for added wave resistance prediction are directly compared by studying the influence of various input parameters, such as advance speed and draught. The main achievement of the paper is a case study focused on the relation between added wave resistance, propeller light running margin, and MPP for three example ships. In the case study, the propeller's operational point is predicted for a given ship in various sea states; thus leading to an assessment of the operational points of the propeller in relation to the load limits of the main engine, and hereby returning a prediction of the forward speed that the ship can maintain in the given sea state. Indeed, the novelty of the study is the combined engineering considering resistance, propulsion, operational conditions, *and* engine loading altogether in a preliminary assessment of MPP for a ship sailing in a given sea state; all of it considered from a practical perspective.

It seems relevant to mention that [7] contains a study that has some similarity to the present work. In [7], the focus is on the need for resistance estimation considering design of ships with special attention to added wave resistance, however, without the particular concerns related to minimum propulsion power and propeller light running margin, as discussed in the present paper.

1.3. Composition of paper

The paper contains five sections in total, and the contents of the four remaining sections are summarised in the following. Section 2 presents the theoretical background and the methodology of the study. Section 3 contains the comparisons of the numerical methods used for the prediction

of added wave resistance. The practical relevance of the study is exemplified in Section 4 by a numerical case study focused on an evaluation of the operational points (power and rpm) in relevant sea states, relative to the engine load diagram, as provided by a designer of two-stroke main engines. Finally, conclusions and suggestions for future research and topics to consider in the legislation are given in Section 5.

2. Theoretical Background and Methodology

This section outlines the basics of added wave resistance on ships together with the numerical methods later compared. The section also includes a description related to the estimation of the *total* resistance on a ship in a seaway. Moreover, the section gives an overview of the most fundamental aspects in connection with ship propulsion. The latter parts, regarding total resistance and propulsion, will be used in the numerical case study focused on an evaluation of minimum propulsion power according to assessment level 2 for given ship design and main engine including the associated load diagram. Note, at most places, the physical parameters and symbols used in the stated formulas are defined in the main text along with the actual mathematical expressions, but for convenience Table 1 summarises the complete list of the most important symbols.

2.1. Predicting added resistance in waves

Added wave resistance on a ship is a result of the forces associated with diffraction and reflection of waves around the hull together with radiation of waves because of ship motions due to the wave excitation loads. The literature about added resistance in waves is wide, and the references [8, 9, 10] are all useful to obtain a sound background on the topic. On the other hand, this paper has no intention to carry out detailed numerical calculations of added wave resistance for what reason reference to the huge special literature, notably on CFD-based studies, is excluded.

Generally, added wave resistance on a ship can be represented by a transfer function $\Phi(\omega)$, which expresses the response per unit wave amplitude as function of wave frequency ω or wave length λ. A qualitative example is shown in Figure 1 where L is the length of the ship and B is the breadth, while ρ and g are the density of water and the acceleration of gravity, respectively. The domain of resistance due to diffraction of the incident wave (bow wave reflections) and the domain of radiation due to ship motions are also roughly indicated in the figure. It is seen that the added

Table 1: Parameters relevant for the estimation of added wave resistance.

Symbol	Description	Unit
$\bar{R}_{AW}$	Mean added wave (AW) resistance	N
$\Phi_{AW}(\omega)$	Transfer function of added wave resistance	N
$S(\omega)$	Wave spectrum density	m^2s/rad
ρ	Water density	kg/m^3
g	Acceleration of gravity	m/s^2
ω	Angular wave frequency (absolute)	rad/s
$\overline{\omega}$	Angular wave frequency (encountered)	rad/s
ζ_A	Wave amplitude	m
λ	Wave length	m
k	Wave number	rad/m
H_s	Significant wave height	m
T_1	Mean wave period	s
L_{pp}	Length between particulars	m
T_M	Draught amidships	m
B	Breadth	m
C_B	Block coefficient	-
Fr	Froude number	-
V_S	Ship's speed-through-water	m/s
r_{yy}	Pitch radius of gyration	m
$I_1(x)$	Modified Bessel function of the first kind of order 1. x is the argument	-
$K_1(x)$	Modified Bessel function of the second kind of order 1. x is the argument	-

wave resistance attains a maximum in the frequency range dominated by radiation of waves due to movements of the ship. Typically, the peak value is found around $\lambda/\mathrm{L} \approx 1$.

Based on the transfer function, it is possible to describe the added wave resistance in an irregular sea using the wave energy (density) spectrum. Thus, if the sea state is described by a wave energy spectrum $S(\omega)$, the mean added resistance $\bar{R}_{AW}$, in the surge direction, can for constant speed and (wave) heading be determined by Eq. (3), cf. [9]. Here, the transfer function $\Phi_{AW}(\omega)$ for the added wave resistance is normalised by the square of the wave amplitude ζ:

$$\bar{R}_{AW} = 2\int_0^\infty S(\omega)\frac{\Phi_{AW}(\omega)}{\zeta^2}d\omega \tag{3}$$

The main concern about Eq. (3) is that the calculation of the transfer function requires detailed information about the considered ships's hull lines, which are rarely available in the design stage in connection with assessment of (minimum) propulsion power. In terms of the MPP-guidelines [1], the requirement is, in fact, one step beyond, since accordingly the transfer function must be obtained from model-scale tests. However, in the early phases of ship design, it is beneficial

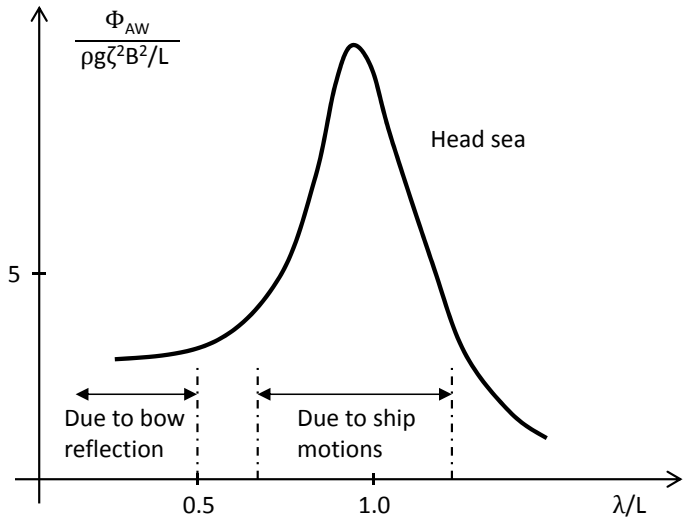

Figure 1: Principal illustration of the non-dimensionalised transfer function for added wave resistance in head seas as a function of the ratio between wavelength and ship length. With inspiration from [9].

to rely on method(s) taking just a limited number of variables as input; for instance, the main particulars of the hull together with a specification of the operating conditions including sea state. In the following, consideration is therefore only given to such formulas, as they may be useful when new ship designs are investigated with respect to (minimum) propulsion power; especially when added wave resistance is the major component as is the case for smaller ships at low to vanishing speed in severe seas. On a side note, it can be mentioned that "intermediate" approaches for predicting added wave resistance exist. Thus, the appendix of [5], taken from [11], contains a method that can be used to determine a quadratic transfer function. This method resembles that of STAwave-2, see below, but requires additional information about the waterline of the vessel. Similarly, the experimentally-based study [12] facilitates a relatively simple formula, derived from regression analysis, for the estimation of added wave resistance when knowledge about the waterline is available (or assumed). In future studies, it should be interesting to include predictions based on these methods. However, in the present work, the actual accuracy, in absolute terms, of the models is not the central topic but rather it is the influence on the calculation of the loading of the main engine, as illustrated in the case study in section 4.

2.1.1. STAwave-2

The STAwave methods 1 and 2, as initially introduced by [13], were developed in order to correct for the effect of waves during sea trials. STAwave-1 corrects only for the reflection contribution to added wave resistance, and it is required that the ship does not pitch nor heave; thus radiation is neglected. Because of this fact, STAwave-1 is not given any further attention in the present study, since adverse weather conditions are of interest only. On the other hand, STAwave-2 considers both reflection and radiation and, as shown below, closed-form expressions are formulated for the transfer functions of both parts.

As mentioned, STAwave-2, e.g. [14, 15], is primarily used for the correction of sea trial data, and thus low Froude number evaluations have not been included in the model tank test scheme upon which the method is developed. Therefore, usability in a study focused on MPP is challenged by a requirement that $Fr > 0.10$. This limitation is *not* set due to physical reasons but, as indicated, due to the omission of data to perform a regression at lower Froude numbers. For the contribution from wave reflection, the lower Froude number is not expected to influence the calculated value: The low(er) encounter frequency, resulting due to low(er) forward speed, is not critical to the magnitude of resistance from reflection as this contribution is constant. For the contribution from radiation, resulting from ship motions, the situation is different as the application of a lower Froude number in the regression equations will shift the peak value of the transfer function towards ratios of $\lambda/L_{pp} < 1$ which is not in line with theory, e.g. [9, 10], nor in line with the original description [13]. One solution to this problem, from a practical point of view, is to include a correction factor that adjusts, i.e. increases, the value of the pitch radius of gyration with decreasing Froude number, in order to "relocate" the peak of the transfer function. This adjustment is nonphysical, but corrects the regression-based transfer function to attain its well-known characteristics with a peak located close to $\lambda/L_{pp} = 1.0$. Despite the non-physical character of this correction, the method of STAwave-2 is included since it is known to have seen application in the industry[‡], even without the correction factor. Clearly, it would be of interest to carry out validation of the corrected estimate with experimental results at low(er) speed. While this is out of scope from the present study, it has indeed interest as a future exercise. In the present study, the consequence of the introduced modification to the STA2 method is investigated from a numerical perspective only; this happens

[‡]This has been observed by the first author in connection with development projects with industrial partners.

in the sensitivity study in Section 3, see also Figure 2, where methodical comparisons are made with the other semi-empirical methods.

As already stated, the STAwave-2 method formulates closed-form expressions for the transfer function for the added wave resistance. Subsequently, the transfer function is combined with a wave energy spectrum to determine the mean added wave resistance. The (parametric) transfer function $\Phi_{AW}(\omega)$ takes the form:

$$\Phi_{AW} = \Phi_{AW,RL} + \Phi_{AW,ML} \tag{4}$$

where $\Phi_{AW,ML}$ is the part due to wave-induced motions while $\Phi_{AW,RL}$ is due to wave reflections. The formulas of the two parts are given by,

$$\Phi_{AW,ML} = 4\rho g \zeta_A^2 \frac{B^2}{L_{pp}} \overline{r}_{aw}(\omega) \tag{5}$$

$$\Phi_{AW,RL} = \frac{1}{2}\rho g \zeta_A^2 B \alpha_1(\omega) \tag{6}$$

The definitions of the individual parameters are listed in the following, and Table 1 contains descriptions of those parameters that have a direct physical meaning:

$$\overline{r}_{aw}(\omega) = \overline{\omega}^{b_1} \exp\left(\frac{b_1}{d_1}(1-\overline{\omega}^{d_1})\right) \cdot a_1 Fr^{1.50} \exp(-3.50 Fr) \tag{7}$$

$$\overline{\omega} = \frac{\sqrt{\frac{L_{pp}}{g}} k_{yy}^{1/3}}{1.17 Fr^{-0.143}} \omega \tag{8}$$

$$a_1 = 60.3 C_B^{1.34} \tag{9}$$

$$b_1 = \begin{cases} 11.0, & \overline{\omega} < 1 \\ -8.5, & \overline{\omega} \geq 1 \end{cases} \tag{10}$$

$$d_1 = \begin{cases} 14.0, & \overline{\omega} < 1 \\ -566 \left(\frac{L_{pp}}{B}\right)^{-2.66}, & \overline{\omega} \geq 1 \end{cases} \tag{11}$$

$$\alpha_1(\omega) = \frac{\pi^2 I_1^2(1.5kT_M)}{\pi^2 I_1^2(1.5kT_M) + K_1^2(1.5kT_M)} f_1 \tag{12}$$

$$f_1 = 0.692 \left(\frac{V_S}{\sqrt{T_M g}}\right)^{0.769} + 1.81 C_B^{6.95} \tag{13}$$

It is noted that the transfer function is given as function of absolute frequency ω. However, implicitly the formulas depend on the vessel forward speed relative to wave propagation (direction and phase velocity of the waves), and the encounter frequency $\overline{\omega}$ is therefore introduced in Eq. (8).

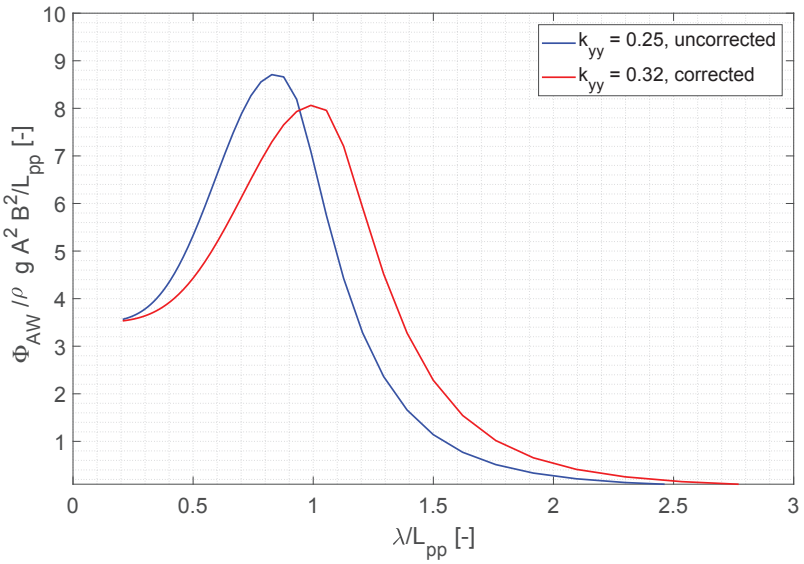

Figure 2: Transfer function estimated by STAwave-2, with and without correction of k_{yy}, for a 27,000 DWT tanker ($L_{pp} = 160$ m) at a speed of 6 knots.

From the formulas, and Table 1, it is noted that the transfer function can be calculated with information only about the main particulars and the non-dimensional pitch radius of gyration $k_{yy} = \frac{r_{yy}}{L_{pp}}$, which often is approximated by $k_{yy} = 0.25$, e.g. [16]. The application of the transfer function is limited to the following conditions, cf. [15]: $L_{pp} > 75$ m, $4.0 < L_{pp}/B < 9.0$, $2.2 < B/T_M < 9.0$, $0.10 < Fr < 0.30$, $0.50 < C_B < 0.90$, and relative wave direction is within 0 deg to $\pm$ 45 deg off-bow, emphasising that the speed restriction is relaxed in the present study by correcting the pitch radius of gyration. An example of the influence of the correction to the pitch radius of gyration is illustrated in Figure 2 for a tanker of $L_{pp} = 160$ m at 6 knots, i.e. $Fr = 0.08$. It can be appreciated that the peak is shifted to a larger wave length, roughly at $\lambda/L_{pp} = 1$. In this context, it is interesting to note that results in [7] in fact suggest that the peak of STAwave-2, in its original formulation without the modification of k_{yy}, also for higher speeds ($Fr \approx 0.15$) likely is located at a too small wave length relative to experimental results and the method developed in [17]. In other words, a finding that indicates a need to shift the location of the peak to a larger wave length which, as seen herein, can be achieved by modifying the pitch gyration radius. Additional discussions about the effect of the correction have been given by [18], and a few remarks are also given in Sections 3 and 4 where results of STAwave-2 are compared to results obtained by the other methods for predicting the mean added wave resistance.

From the transfer function given in Eq. (4), the mean resistance increase due to long-crested head waves is given by Eq. (3). Note that any increased usage of the rudder in adverse conditions is not accounted for.

2.1.2. SHOPERA

The SHOPERA project was launched by the EU in response to the implementation of EEDI and associated concerns on MPP. The estimate of added wave resistance, developed as an outcome of the SHOPERA project, is in this study included in a modified form proposed to the MEPC in [5]. The formula for the mean added resistance in waves is given by,

$$\bar{R}_{AW} = 1336(5.3 + V_S)\left(\frac{B \cdot T_M}{L_{pp}}\right)^{0.75} H_s^2, \qquad \text{[N]} \tag{14}$$

where the parameters are defined in Table 1. The details of the empirical relation are given by [6], but it is noteworthy that the formula is based on numerical evaluations of transfer functions using a Rankine panel method for resistance estimates of 50 bulk carriers, tankers and general cargo ships with main particulars limited by: 90m $< L_{pp} <$ 320m, $5.0 < L_{pp}/B < 7.9$, $2.0 < B/T_M < 3.3$, $0.78 < C_B < 0.87$. In addition, the following constraints apply: $0 < V_S < 8.0$ knots, and relative wave direction is within 0 deg to $\pm$ 30 deg off-bow.[§] To calculate the magnitude of the added resistance, a JONSWAP wave spectrum has been used by [6]. No direct explanation is given to this choice but, in general, focus in the project is/was on a ship's capability to weather-wane in areas close to the coast and, hence, it makes sense to consider a fetch-limited ocean wave spectrum.

As indicated by the constraints on the hull-parameters, the method of SHOPERA is established based on a regression of simulation results of hulls of very specific characteristics focused on tankers and bulk carriers. These ship types are accessed most likely to experience problems with MPP under the EEDI-scheme, and the calculations (and the resulting formula) are based on ships designed to fulfil EEDI phase 2, [6]. It is clear that the accuracy of the Rankine code is fundamental to the reliability of the formula, cf. Eq. (14). [19] has studied the performance of the specific code and make an evaluation of the motions predicted on deep water while [20] performs an evaluation of the motions predicted on shallow water. Both studies find good correlation to experimental results. However, as noted by [21], prediction of ship motions is only one step towards predicting the added

[§]In fact, [6] specifies $\pm$ 60 deg, while $\pm$ 30 deg is the range given in [5].

wave resistance, and a good prediction of the motions themselves does not necessarily guarantee a good resistance estimate. A comparison of Eq. (14) with actual operational data is therefore highly relevant, although this is left as a future exercise.

An important addition to Eq. (14) is the inclusion of added resistance arising from an increased usage of the rudder required to keep the course during adverse weather conditions. The magnitude of resistance from increased rudder usage, also known by *steering resistance*, is simply given as a function of the delivered thrust T, cf. [5],

$$R_{rud} = 0.03T \tag{15}$$

The SHOPERA method is as such the only method of the three methods included in the present study, which specifically includes an increase of steering resistance in heavy weather. It is noteworthy that the 'SHOPERA estimate' is stated to be conservative [6]. Thus, the result of Eqs. (14) and (15) in combination is adjusted to return values greater than the individual results of the numerical simulations upon which the method is based.

As a final remark - and as a word of caution - about the empirical formula expressed by Eq. (14), it is a concern that the right-hand side of the equation is not dimensionally consistent. This makes it difficult to properly assess the equation with regards to its physical variables and their influence on the value of the result. It is not the role of the authors to criticise this problem, but it is remarkable that the analysis of the data upon which the equation has been based is not reflecting a rigorous dimensional analysis [22]. ¶

2.1.3. DTU Design Tool

The main purpose of the computational tool is to make potential flow calculations available in the early phase of new ship designs. All the details of the tool are given in [23, 24], and the following is just a brief outline.

The tool takes as inputs the ships's main dimensions: length L_{pp}, breadth B, draught T, together with the block coefficient C_B and advance speed V_S. Based on these inputs, the tool interpolates linearly in a large set of pre-calculated transfer functions computed using potential flow calculations on a series of reference geometries in the range of length-to-breadth ratios $4.0 <$

¶The discussions with an anonymous reviewer about the Buckingham PI theorem (used for dimensional analysis) is appreciated.

$L_{pp}/B < 8.0$ and breadth-to-draught ratios $2.0 < B/T_M < 5.0$. The reference calculations have been performed at a range of Froude numbers from 0 to 0.25, in between which linear interpolation is performed for the exact Froude number based on the ship's actual speed and length. The tool applies two different methods to determine the transfer function for added wave resistance depending on the ratio between the encounter-wave length and the length of the hull: For relatively long waves, Salvesen's method [25] is applied, and for shorter waves Faltinsen's asymptotic method [26] is used.

It is noteworthy that the tool can be inaccurate at near zero forward speed and in beam to following seas, cf. [25]. Specifically, this situation may occur if the body potential is not small compared to the potential of the incident wave. According to [1], the ship speed is required not to drop below 4 knots, and, as only head (to beam) seas are considered, the tool is expected to be sufficiently accurate; at least for application within a study focused on MPP. It is also worth noticing that Faltinsen's asymptotic method is sensitive to the shape of the bow, and returns the highest values for blunt bow shapes. The DTU Tool does not account directly for this but, based on the block coefficient provided as input, the tool interpolates in high and low C_B-databases of hulls with bow-shapes typical for the given block coefficient.

In order to calculate the mean added resistance, the (interpolated) transfer function must be combined with a wave spectrum, cf. Eq. (3), and the tool offers a choice between a Bretschneider and a JONSWAP spectrum together with inputs of significant wave height and a characteristic wave period such as the mean or the zero-upcrossing period.

2.2. Estimating the total resistance on a ship in a seaway

The total resistance exerted on a ship sailing in waves is the sum of the calm-water resistance and a number of extra contributions, including added wave resistance, that occur because of various phenomena. Together with the added wave resistance, the additional resistance components are: Wind resistance, increased steering resistance, and possibly shallow water effects. Furthermore, hull fouling and stabilizer fins, if present/applied, leads to an increase in the total resistance. In principle, *all* resistance components should be included when estimating the necessary propulsion power of a ship. However, focusing explicitly on *minimum* propulsion power, the guidelines [1] consider just the calm-water resistance with the hull as in sea trail condition, and added resistance from wind and waves. The reason is that ship speed is low to vanishing and, as a result, these

components are usually the most relevant; especially for the considered segments of ship types and sizes (bulk carriers and tankers). The calculation methods for added wave resistance were presented in the preceding sections. Below, a few remarks about the calculation of the calm-water resistance and the wind resistance are given.

2.2.1. Calm-water resistance

For a given ship, it is common practice to calculate the calm-water resistance by use of model-scale towing-tank tests, as suggested in the ITTC-1978 Method, e.g. [27]. If towing-tank tests are not available, like in the early design phase of a ship, alternative methods can be applied to estimate the calm-water resistance, as suggested by [28] and [29]. In the present study, the calm-water resistance is predicted by the method by [28], estimating the calm water resistance based on a series of regression based coefficients, taking input on main particulars, length-displacement ratio, and the prismatic coefficient. Effects of the position of the longitudinal centre of buoyancy is neglected in this consideration of the early design stage. In the present study, the updated coefficients as established by [30, 31] has been implemented for the calculation of the coefficients to reflect statistics for more recent ships. Note that the estimate by [28] as applied in the present study, includes frictional resistance, air resistance, appendage resistance, steering resistance and residual resistance composed of wave making resistance and viscous pressure resistance.

2.2.2. Wind resistance

The wind resistance depends on the relative wind speed and direction, and the projected windage area of the ship. In this study, the calculation follows the standard ISO-15016 [15], calculating the wind resistance by the effective area of the super structure and a wind resistance coefficient, both calculated as a function of the relative wind direction, though here only considering head wind as part of the simplified assessment. Data on wind resistance coefficients and super structure areas for different ship types and sizes are calculated by the regressions given by [32, 33].

2.3. Ship propulsion and engine loading

2.3.1. Operational point and propulsion coefficients

In a context of MPP assessment, the aim is to determine the location of the (directly coupled) main engine's operational point corresponding to the total resistance. In other words, it must be assessed if the required rate of revolutions of the FP propeller and the corresponding brake power,

as a pair, lies within the load diagram of the intended engine. One possible approach to make this assessment is suggested in the following, where the basic principles of ship propulsion are taken from [34]. It is assumed that the propeller design is approximated by the Wageningen B-series [35] in order to be able to relate the propeller coefficients K_Q and K_T in the open-water diagram. A propeller with diameter D and rate of revolutions n is considered, the density of water is ρ.

The total resistance R_{tot} on a ship with given main particulars and for specified operational conditions, including waves and forward speed, can be estimated as outlined in subsection 2.2. In this case, the required thrust T is given by,

$$T = \frac{R_{tot}}{1-t} \tag{16}$$

where t is the thrust deduction coefficient, which can be estimated from the method by [36], later updated by [30]. The same reference(s) may also be used in the estimate of the wake fraction coefficient $w = V_w/V_S = (V_S - V_A)/V_S$, where V_S is the ship's speed (through water), and V_w is the wake velocity while V_A is the velocity of water arriving at the propeller. Alternatively, values for t and w are suggested by [1]. The advance coefficient $J_A = V_A/(nD)$ and the thrust coefficient K_T are unknown, implying that the required torque Q is neither available. By definition, $K_T = T/(\rho n^2 D^4)$ which can be rewritten,

$$\frac{K_T}{J_A^2} = \frac{T}{\rho V_A^2 D^2} \tag{17}$$

As the ratio on the right-hand side is known (i.e. can be calculated), the K_T-identity [36] means that unique solutions for K_T and J_A, respectively, are available for every value of thrust and corresponding speed (V_A); keeping in mind that the propeller design is approximated by the Wageningen B-series. Consequently, the torque coefficient K_Q can subsequently be directly inferred from the open-water diagram and, since the rate of revolutions n is available through the advance number, i.e. $n = V_A/(J_A D)$, the brake power becomes,

$$P_B = \frac{2\pi n K_Q}{\eta_s \eta_r} \tag{18}$$

where η_s and η_r are the shaft efficiency and the relative rotative efficiency, respectively. Altogether, the prediction of n and P_B completes the determination of the location of the operational point of the main engine. The practical relevance of this approach, in relation to MPP, is exemplified in the case study presented in Section 4.

It is noteworthy that, in this study and like in [1], it is assumed that the wake fraction coefficient w and the thrust deduction factor t, as obtained for calm-water conditions, are applicable also in cases of adverse weather conditions, since quasi-steady conditions are assumed with no account for dynamic effects. The accuracy of this assumption can be questioned as discussed by, e.g., [37]. The reason is that the thrust deduction factor will change with the propeller loading, but the error of this is argued to be smaller than the uncertainty of the estimate of t. Other studies, e.g. [26], also discuss the effect of propeller loading on the thrust deduction and wake fraction, and it should be of interest to look further into the effect in future work. Furthermore, the assumption of quasi-steady conditions excludes considerations on dynamic variations in the inflow velocity V_A (and hereby dynamic variations in the resulting thrust T) and any possible influence of this towards the dynamic response of the main engine.

2.3.2. Engine load limits

In this study the static load diagram of the typical prime mover of larger merchant vessels, a low speed two-stroke engine is considered. The static load diagram by one of the designers of such engines [34] expresses a combination of power and speed limits, the most relevant for considerations of MPP, the so called "torque limit", limiting an engine's capabilities with respect to heavy running. The torque limit is mainly applied to reduce the thermal load, and thereby thermal wear rates, on combustion chamber components, such as the fuel injection valves, piston crown, and exhaust valve spindle, in order to attain satisfactory service intervals. Traditionally, the torque limit has predominantly been depending on the actual mechanical limits of the engine, especially considering the maximum pressure permitted on the bearings. However, this dependency is less clear for a modern engine with electronic control of the fuel injection, permitting control of the maximum pressure attained during combustion while running heavy. The power limits of the load diagram are imposed by limits to the amounts of fuel injected per revolution, expressed by an index of the amount injected at 100% engine load and speed.

In line with the requirements of [1], only the static load diagram and mean added wave resistance is considered in the present study, even if dynamic limits to the fuel index exist: In relation to MPP, the most relevant part of the dynamic fuel limits is the so-called "scavenge air limit", which limits the fuel index based on the scavenge air pressure. The scavenge air (fuel index) limit reflects the amount of air available for combustion and limits the fuel index accordingly in order to reduce

the soot formation. Hence, this fuel index limit may restrict the amount of fuel injected in a (real) dynamic seaway. To exemplify, consider the case of propeller ventilation where the load on the engine reduces, requiring a reduced fuel injection in order to avoid over-speeding, typically attaining zero fuel index. This results in a lowering of the mass flow across the turbo charger, which in turn leads to a reduction of the scavenge air pressure and thereby the fuel index permitted. The scavenge air (fuel index) limit increases as the turbocharger is accelerated once the engine load increases upon submergence of the propeller. This can potentially limit the fuel index permitted resulting in a lowering of the engine speed until reaching a scavenge air pressure corresponding to the fuel index required to maintain the engine speed set point. In a dynamic seaway this will lead to variations in the engine speed.

In addition to limitations on the fuel index imposed by the resulting lower scavenge air pressure after a propeller emergence, propeller emergence may involve a risk of turbo charger surging. Continuous operation with a surging turbo charger[‖] is to be avoided but operation in conditions so severe that full propeller emergence occurs with resulting risk of surging, is not considered continuous operation, similar e.g. to surging resulting from a crash-stop with a sudden reduction of fuel injection [38].

3. Comparisons of Estimates of Added Wave Resistance

Three semi-empirical methods for predicting added wave resistance were presented in Subsection 2.1. In the present section, a sensitivity study will be undertaken considering the influence of different operational conditions. As described previously, fulfilling the requirements for minimum propulsion power is most challenging to the design of smaller ships. In this light, the sensitivity study is focused on results for a 11,000 DWT tanker, a 27,000 DWT tanker, and a 50,000 DWT tanker, where the latter is included to cover a common MR tanker. All three ships have been assessed to be capable of fulfilling EEDI phase 2. Main particulars of the considered ships are provided in Table 2. A few practical remarks are worth noticing:

- The results of the prediction methods will be referred to by the following abbreviations; results of STAwave-2 are denoted by 'STA2', the method of SHOPERA and its results are

[‖] Continuous surging typically happens due to insufficient cleaning resulting in clogging of both the compressor and turbine parts, insufficient maintenance, insufficient air supply to the engine room or faulty fuel injections, etc.

Table 2: Particulars of the tankers for theoretical evaluations of the methods for predicting added wave resistance all with 15% sea margin, 10% engine margin, 5% propeller light running margin and a specified maximum continuous rating (SMCR) as given

Capacity [DWT]	11,000	27,000	50,000
Length L_{pp} [m]	112	152	176
Breadth B [m]	20	27	32
Draught T_d [m]	7.5	10	11
T_d/L_{pp}	0.067	0.066	0.063
Block coef. $C_{B,Lpp}$ [-]	0.73	0.73	0.80
Design speed V_d [knots]	14.5	14.5	14.7
SMCR-kW	4,000	5,700	7,300
SMCR-rpm	160	108	89
Prop. diameter D_{prop} [m]	4.2	5.8	6.8
Blade number N	4	4	4
Area ratio Ae/Ao [-]	0.55	0.55	0.55
Pitch diameter ratio $P/D_{0.7}$ [-]	0.772	0.775	0.745

'SHOP', and the results from the DTU Design Tool are referred to as 'DTU Tool' or 'DTU' when given in figure legends.

- All methods are proportional to H_s^2, and results are shown just for $H_s = 1$ m.
- The additional steering resistance, cf. Eq. 15, associated with the SHOPERA equation is *not* included, so to have an equal basis for the three methods.
- Finally, the wave spectrum is taken as a Pierson-Moskowitz spectrum which is a special case of the JONSWAP spectrum when the wind speed is related to significant wave height. The spectral formula(s) can be found in any standard textbook on naval architecture or ocean engineering, e.g. [39].

The results of the sensitivity study are presented in Figure 3 which shows the variation of predicted added wave resistance as function of advance speed V_S, draught amidships T_M, and mean wave period T_1. In any one case, the two other parameters are constant and their values are indicated; noting that the values are set somewhat arbitrarily albeit they reflect [1]. The main findings from the plots are summarised as follows. Generally, there appear large deviations between the predictions, and it is only possible to find a sort of "best agreement" between the results for specific values or, at best, for very small intervals of the studied parameters (V_S, T_M/T_d, T_1). It is also noted that the trends of the three predictions are quite different; STA2 and SHOP increase

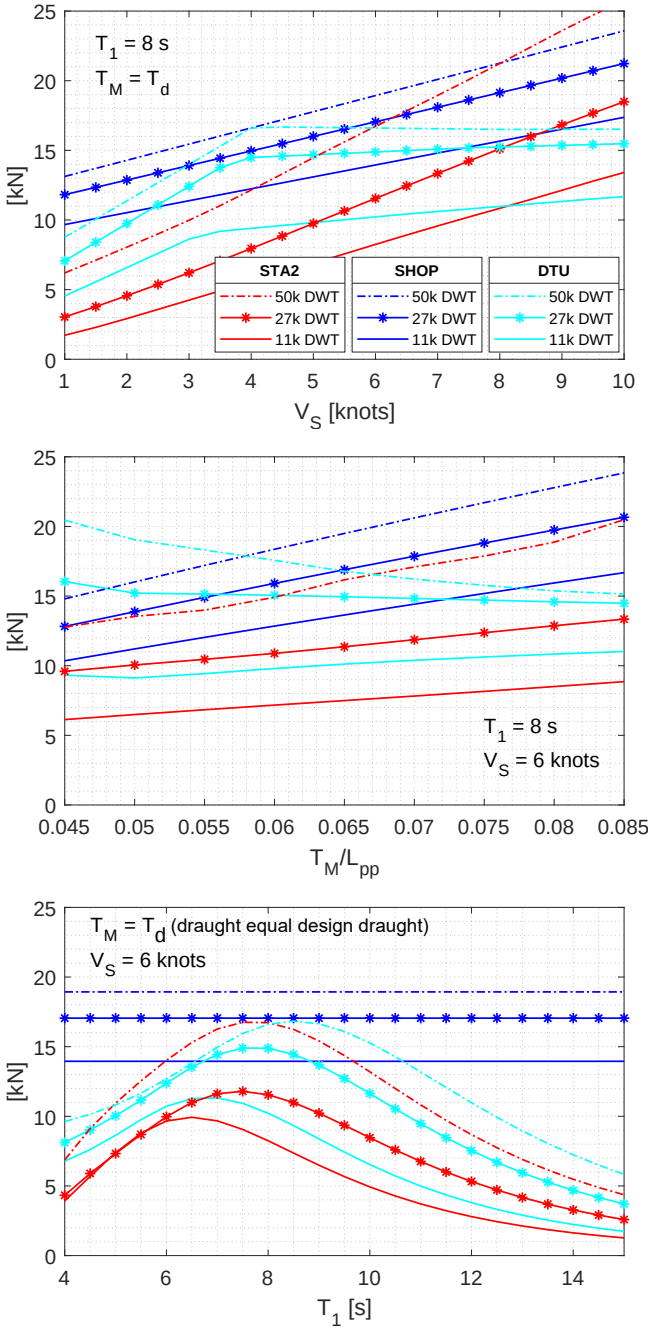

Figure 3: Theoretical predictions of added wave resistance. Upper plot: Variation with advance speed. Middle plot: Variation with (non-dimensional) draught; the non-dimensional *design* draught is app. 0.065 for all three ships. Bottom plot: Variation with mean wave period T_1. The legend in the top plot applies also to the other two plots.

both linearly with speed and draught on the studied intervals, while the behaviour of the DTU Tool for these parameters has more details. On the other hand, there is a similar behaviour of STA2 and the DTU Tool when a variation in the wave period is considered; while, in this case, SHOP is invariant to changes. In addition to the overall findings, some specific remarks are listed in the following.

Variation with speed: The discontinuity of the DTU Tool is the result of the difference in the methods applied depending on encounter frequency (or wave length); Salvesen's method vs. Faltinsen's asymptotic method. The STA2 prediction method is originally developed for sea trial corrections, and has a lower speed limit for its application; $Fr = 0.1$ has been set, which correspond to 6.4 knots, 7.5 knots, and 8.1 knots for the 11,000, the 27,000, and the 50,000 DWT ships, respectively. In principle, it is therefore beyond the validity of STA2 to select the speed as $V_S = 6$ knots as done when draught and wave period are varied. However a correction to the pitch radius of gyration has been implemented, as described in Section 2.1.1, in order to include the consequences of extending the model towards lower Froude numbers.

Variation with draught: The conflict in increasing and decreasing trends of the predictions (STA2 and SHOP vs. DTU) is observed because of the underlying methods. The STA2 method is based on an empirical analysis of an extensive series of model-scale tests, the SHOPERA equation is based on a series of evaluations by a Rankine source method, and the DTU Tool is based on potential flow theory. For the latter, when predicting added wave resistance by potential flow theory, the motions of the ship and hereby radiation of waves, is a significant contribution to the total added resistance. At lower draughts, the motions of the ship are expected to be relatively larger, which will increase the added resistance predicted by potential flow theory. In addition, both SHOPERA and STAwave-2 treats waves up to 30 deg and 45 deg off-bow, respectively, as head waves, which might provide an explanation why the methods in general are less sensitive to ship motions.

Variation with wave period: The maximum added wave resistance for STA2 and the DTU Tool occurs in an interval of 7-8.5 s of the mean wave period. The actual value depends on ship length, but it is seen that the SHOPERA equation takes a larger (constant) value in all cases. This is not surprising as the intention of the SHOPERA equation is to return a conservative prediction corresponding to a wave period that will result in $\lambda/\mathrm{L} \approx 1$, where added resistance is largest.

Table 3: Maximum speeds attainable in "worst case" wave period as per the methods applied for predicting added wave resistance, for sea states corresponding approx. to Beaufort 7, 8 and 9 with 5% propeller LRM.

Capacity [DWT]	11,000	27,000	50,000
Speed attained	[knots]	[knots]	[knots]
SHOPERA, $H_s = 4$ m	7	9.5	10
STAwave-2, $H_s = 4$ m	9	11	9.5
DTU Tool, $H_s = 4$ m	11.5	12.5	11.5
SHOPERA, $H_s = 5.5$ m	-	1	3
STAwave-2, $H_s = 5.5$ m	4.5	5.5	5
DTU Tool, $H_s = 5.5$ m	1.5	2.5	3.5
SHOPERA, $H_s = 7$ m	-	-	-
STAwave-2, $H_s = 7$ m	2.5	5.0	2
DTU Tool, $H_s = 7$ m	-	-	1

Although not shown, it is interesting to note that if the speed drops to 4 knots there is an exact match between the result of the SHOPERA equation and the maximum of the DTU Tool.

Based on the (theoretical) comparisons between the methods for added wave resistance prediction, it has been seen that an evaluation of minimum propulsion power and testing of compliance will be dependent on the method chosen. This is exemplified in the next section.

4. Case Study on Effect Towards Minimum Propulsion Power Compliance

In the following case study, an example evaluation of whether a ship design with a specific propulsion plant fulfils the MPP requirements or not is illustrated. The example combines the methodology for determining resistance on the hull and application of the various methods for determining the added wave resistance together with the method for determining the operational point of the FP propeller, as described in Section 2.3. The study presents the detailed results for the 50,000 DWT MR tanker, cf. Table 2, but results for all three ships are summarised in Table 3.

4.1. Results in rule-determined sea state

In Figure 4, the operational points of the main engine are illustrated for various ship speeds in the rule-defined sea state [1], that is, $H_s = 4$ m with corresponding wind speed of $V_{wind} = 15.7$ m/s; noting that all three ships have $L_{pp} < 200$ m. This sea state corresponds approximately to Beaufort 7. The single operational points are indexed by (integer) numbers that indicate the attainable speed in knots, thus enabling a direct evaluation of the attainable speed, when the mean added resistance

is calculated by the different methods (SHOP, STA2, DTU). Note that the results, in line with the IMO guidelines [1], only represent engine loading as a result of the mean added wave resistance. However, dynamic fluctuations of the operational point of the engine for a given ship speed must be expected, partly because of variations in the instantaneous added wave resistance experienced on the hull, and partly due to wake variations and potentially dynamic propeller ventilation. Such dynamic fluctuations are not considered in the guidelines, and this constitutes a weak point of the simplified assessment of mean added wave resistance; simply because no attention is given to the dynamic limits of the main engine and to dynamic effects, e.g. resulting from a reduction of scavenge air pressure after a ventilation.

It is noteworthy that in the considered sea state, the operational propeller curves resulting from the mean added resistance predicted by the methods of SHOPERA and STAwave-2 are so heavy that the engine is prohibited from reaching 100% speed and thereby also prohibited from delivering 100% power continuously. This illustrates that the minimum speed a ship can maintain during adverse weather conditions is not limited by the maximum power of the engine; rather the ship speed is limited by the torque that the engine can deliver at speeds below 100% speed

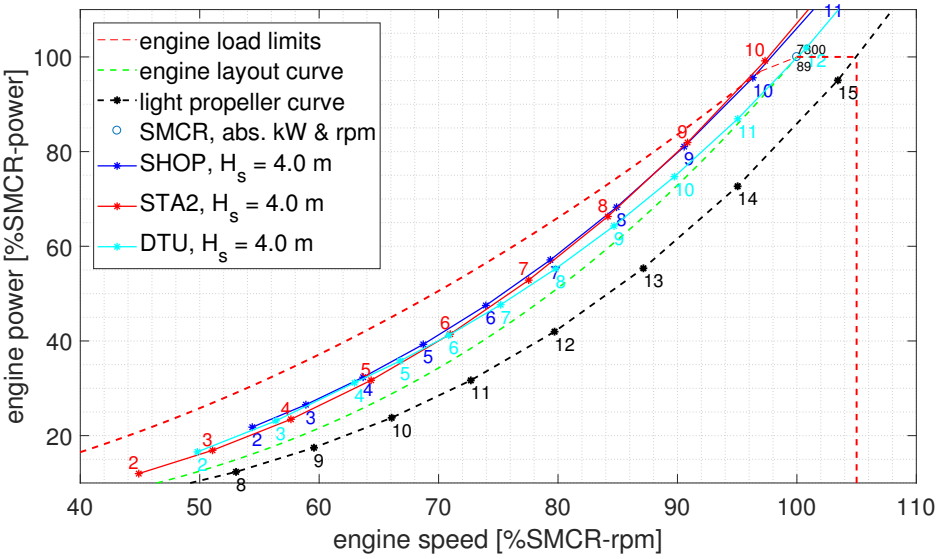

Figure 4: Operational points of the main engine plotted on the engine load diagram [34] as calculated by various methods for the rule-defined sea state ($H_s = 4$ m) and 5% LRM. Integers along curves represent the corresponding ship speed attained.

while operating on a heavy propeller curve. This effect of the engine torque limitation further illustrates the necessity of a propeller light running margin. Thus, the propeller light running margin increases the margin between the light propeller curve and the engine load limits, which, in the end, raises the sea states in which the engine can deliver 100% power. This is given further attention in Section 4.3.

It is of interest that even for a relatively low main engine power of 7,300 kW installed on the ship with 5% propeller light running margin (LRM), the tanker is by all methods estimated to be able to maintain at least 9 knots of forward speed. Under the scheme of [1], 9 knots is the highest value of the minimum course-keeping speed that can be required for a ship design under any circumstances. This is a remarkable difference to the results of assessment level 1 of the IMO guidelines [1], which for a tanker of 50,000 DWT would require 9,220 kW of engine power, without any consideration of the propeller light running margin.

In addition, the change in the relative difference between the attainable speeds and operational points of the main engine, when the added wave resistance is calculated as per the different methods, is quite remarkable: At elevated speeds above approx 7 knots ($Fr = 0.86$), good agreement is found between SHOPERA and STAwave-2. On the other hand, at lower speeds, the relatively best agreement is found between SHOPERA and the DTU Tool; for instance, at 2 knots, SHOPERA predicts 22% SMCR-power at 54% SMCR-rpm, while the DTU Tool predicts 16% SMCR-power at 54% SMCR-rpm. Contrary, at 2 knots, the method of STAwave-2, including the correction to k_{yy} as described in Section 2.1.1, predicts only 12% of the SMCR-power at 45% SMCR-rpm. A remarkable difference indicating that the correction proposed is not sufficient to apply STAwave-2 below the original threshold of $Fr = 0.1$.

The effects of the correction to k_{yy} applied for STAwave-2 are most critical at low Froude numbers, although the effect remains small at $H_s = 4$ m. However, the effects will be more dominant in increasing sea states, and, at $H_s = 7$ m, the difference in the required power is larger than 2% SMCR-power for calculations with and without the correction. For longer ships, attaining even lower Froude numbers, the effect of excluding the correction to k_{yy} is expected to be greater.

The effects of the change between Salvesen's method [25] for longer waves and Faltinsen's asymptotic method for shorter waves [26], see Figure 3, are clearly identifiable in the operational propeller curve predicted by the DTU tool. This results in a degree of propeller heavy running sim-

ilar to SHOPERA at 4-5 knots, while at higher speeds, the resulting propeller curve is significantly lighter than predicted by SHOPERA.

As the extent of propeller heavy running is decisive to the power that can be delivered and hereby attainable ship speed, small differences amongst the added wave resistance predicted can result in rather large differences in predicted ship speed. However, it is remarkable that the actual extent of propeller heavy running is not that different amongst the methods. With respect to an evaluation according to the IMO guidelines [1], it is instead of interest that the speeds predicted along the propeller curves illustrated in Figure 4 and 5 are so different, as is also shown in Table 3.

Considering this, along with the fact that the difference between the slope of the engine load diagram and the predicted operational propeller curves is rather limited, it is evident that an accurate prediction of the added wave resistance is important even in the early design phase. Therefore, further developments of simplified methods for predicting added wave resistance at an early stage of the design are recommended, in order for the designer to optimise the propulsion plant.

The small difference in slope between the engine load diagram and operational propeller curve also indicates a potential challenge of assessment level 2 in [1]. Thus, even if model tank tests are utilised to determine the transfer function of added wave resistance for the final assessment, small inaccuracies in the development of the transfer function may have a major impact on the actual performance of the ship. On the other hand, the small difference in slope, comparing the heavy propeller curve and torque limit of the engine load diagram, indicates that even small extensions of the engine load diagram can have significant positive effects towards the minimum speed attainable.

4.2. Results in sea state beyond rule requirements

In general, the attainable ship speeds predicted when applying the various methods for estimating added wave resistance in more severe sea states than $H_s = 4$ m vary strongly, as illustrated in Figure 5: For $H_s = 5.5$ m and $V_{wind} = 19$ m/s (Beaufort 8), a maximum speed of 5 knots is predicted by STAwave-2, whereas SHOPERA predicts 3 knots, and the DTU Tool estimates 3.5 knots. These speeds are close to the minimum navigational ship speed of 4 knots as defined per [1].

In significantly adverse conditions, e.g., $H_s = 7.0$ m and $V_{wind} = 25$ m/s (Beaufort 9), see

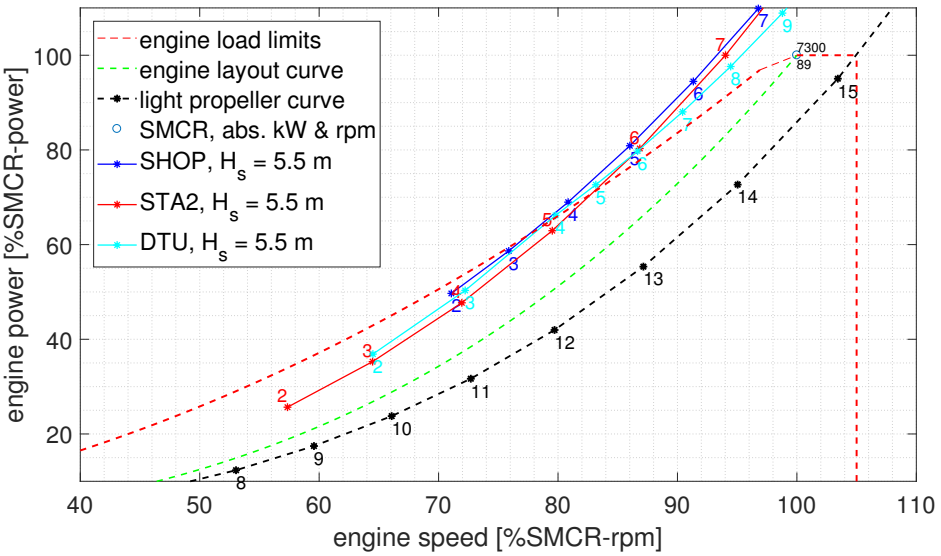

Figure 5: Operational points of the main engine plotted on the engine load diagram [34] as calculated by various methods for $H_s = 5.5$ m and 5% LRM. Integers along curves represent the corresponding ship speed attained.

Figure 6, STAwave-2 and the DTU Tool predicts the operational point of the propeller and main engine to lie within the engine load diagram for a ship speed of 2 knots and 1 knot respectively. At such low speeds, the ship is expected to loose manoeuvrability. It is predicted by SHOPERA that the ship cannot attain a forward speed in this condition.

4.3. Effect of a reduction of propeller light running margin

The propeller LRM has been set to 5% for all three ships considered in the case study, cf. Table 2, and the light propeller curve with 5% LRM was illustrated in Figures 4 to 6. With 5% LRM the pitch is reduced to such an extent that, when operating along the calm water propeller curve in calm waters and with clean hull as in sea trial condition, 100% engine power is delivered at 105% engine speed. This LRM ensures some distance between the light propeller curve and the engine load limits, in order to be able to accommodate some propeller heavy running, i.e. increased propeller load as a consequence of added resistance from fouling or from wind or added wave resistance [34].

If the propeller LRM is reduced to 2% either per design, or if the hull is heavily fouled, significant changes to the attainable ship speed are attained as summarised in Table 4. In $H_s = 4$ m,

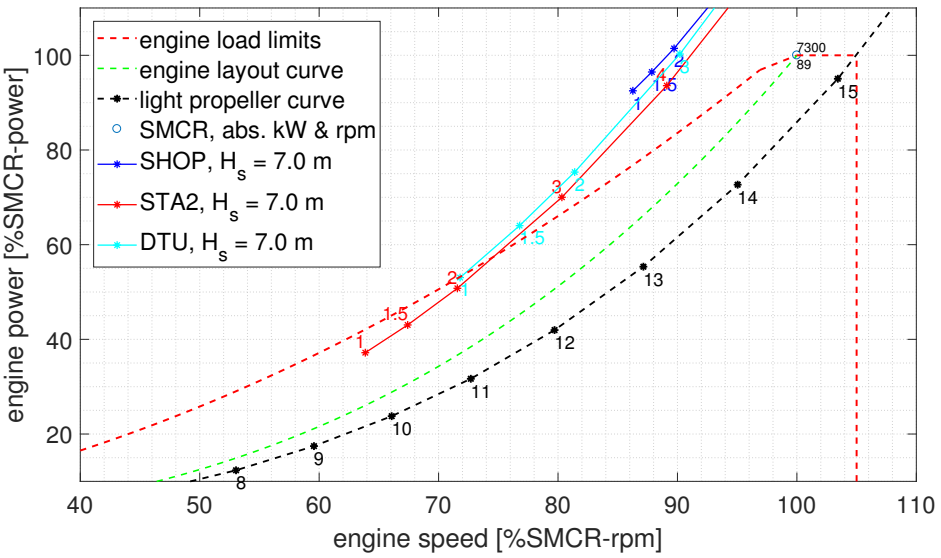

Figure 6: Operational points of the main engine plotted on the engine load diagram [34] as calculated by various methods for $H_s = 7$ m and 5% LRM. Integers along curves represent the corresponding ship speed attained.

Table 4: Maximum speeds attainable in "worst case" wave period as per the methods applied for predicting added wave resistance, for sea states corresponding approx. to Beaufort 7, 8 and 9 with just 2% propeller LRM.

Capacity [DWT]	11,000	27,000	50,000
Speed attained	[knots]	[knots]	[knots]
SHOPERA, $H_s = 4$ m	6	7.5	8.5
STAwave-2, $H_s = 4$ m	8	9	8.5
DTU Tool, $H_s = 4$ m	10.5	12	11
SHOPERA, $H_s = 5.5$ m	-	-	1
STAwave-2, $H_s = 5.5$ m	4	4.5	4
DTU Tool, $H_s = 5.5$ m	1.5	2	3
SHOPERA, $H_s = 7$ m	-	-	-
STAwave-2, $H_s = 7$ m	1.5	2	1.5
DTU Tool, $H_s = 7$ m	-	-	-

the reduced LRM reduces the attainable speed by $0.5 - 1$ knot, compared to results in Table 3, depending on the method applied to estimate the added wave resistance. It is noteworthy that, at $H_s = 5.5$ m and with an LRM of 5%, the attainable forward speeds are just around the minimum navigational speed of 4 knots as defined by [1]. However, with 2% LRM the speed is by SHOPERA

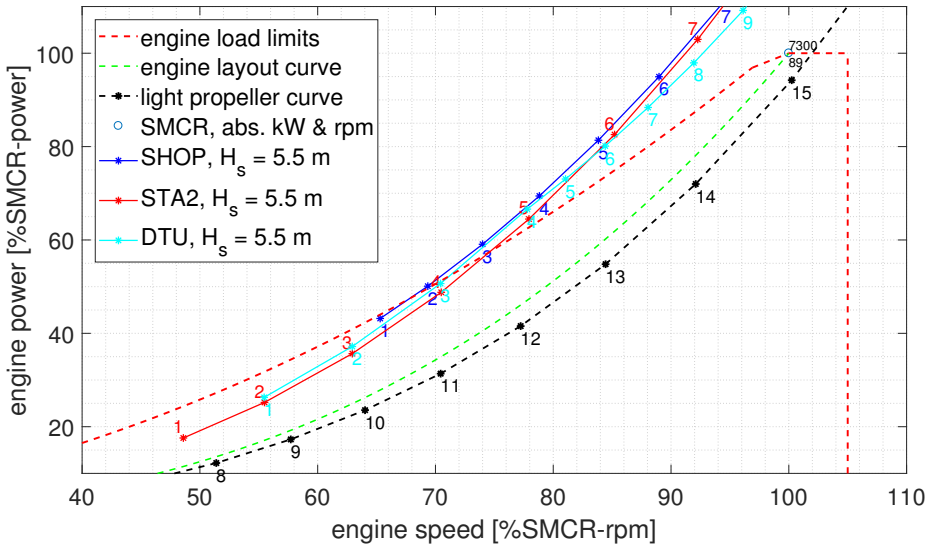

Figure 7: Operational points of the main engine plotted on the engine load diagram [34] as calculated by various methods for $H_s = 5.5$ m and only 2% LRM. Integers along curves represents the corresponding ship speed attained.

estimated to be significantly lower, see Figure 7 compared to Figure 5. For future ships of even lower SMCR, this highlights the importance of the LRM.

In the case of only 2% LRM, the predicted operational points of the engine moves closer to the engine torque limit, increasing the risk that dynamic fluctuations in the added wave resistance will push the actual operational point to the limit. In this case, engine speed will drop and the dynamic load limits of the main engine must be considered to evaluate if the engine and propeller in a moment of lesser added wave resistance can be accelerated back to the desired speed set point and ship speed. Such evaluations have not been performed here. Similarly, other engine types than low speed two-stroke engines may have other load diagrams, extending or limiting such an engine's heavy running capability. Load limits of other engine types, e.g. four-stroke engines, have not been considered.

5. Summary and Conclusions

EEDI requirements have increased the focus on the capabilities of ships to maintain safe manoeuvring speed in adverse weather. In fact, the resulting risk of under-powered newly designed

ships has led the IMO to provide guidelines on minimum propulsion power. As part of the assessment, formulated by the guidelines, stands the estimation of the added wave resistance as a critical and important contribution.

In this paper, three semi-empirical methods for estimation of the added wave resistance have been evaluated in a comparative study targeted on an evaluation of minimum propulsion power at an early design stage. Herein, the influence of ship speed, wave period, and draught has been considered. Two of the evaluated methods, SHOPERA and STAwave-2, predict a (nearly) linearly increasing added wave resistance with ship speed and draught. The third method, the DTU Design Tool, predicts a stepwise linearly increasing added wave resistance with ship speed, while the tool's dependency on draught depends on ship size. The variation with wave period is similar for STAwave-2 and the DTU Tool, albeit the absolute results are quite different. The SHOPERA method is invariant to changes in the wave period.

Focusing on lower speeds, as considered in a case study on minimum propulsion power for three example ships, the absolute difference of the added wave resistance predicted by the various methods may appear relatively small. However, when extending the comparative study further to consider the effects of the added wave resistance predicted towards the loading of the propeller, even small differences become important. For a ship with a typical propulsion plant, consisting of an FP propeller directly coupled to a two-stroke main engine, it is shown that the minimum speed that the ship can maintain during adverse weather conditions is not limited by the maximum power of the engine; rather the speed is limited by the torque that the engine can deliver at lower rpm-ranges. Hereby, small changes in the predicted added wave resistance become of importance as this has influence on the propeller loading and hence the rpm at which the propeller and engine operate. This also indicates that potential efforts into lifting the torque-limit of two-stroke engines will have a large impact on the minimum speed attainable.

The predicted operating rpm affects the power that the main engine can deliver, and ultimately the speed that can be maintained in adverse weather. This is further underlined by the effects of the propeller light running margin, which is shown to have crucial influence on the attainable speed during adverse conditions. In the specific case study, it is noteworthy that even for the most conservative of the methods used for estimation of the added wave resistance, i.e. the SHOPERA method, it appears that there is a good margin for further power reductions before the example

ships cannot meet the requirements of the IMO, as long as adequate propeller light running margins are considered.

The focus of this study has been placed solely on fixed pitch propellers. In the future, the magnitude of efficiency advantage of FP propellers over controllable pitch (CP) propellers may decrease: Potential excessive increases of LRM by pitch reductions, to increase the margin towards the engine load limits, will potentially decrease FP propeller efficiency in the design condition. A potential for attaining a large LRM, without the efficiency penalty of a pitch reduction, lies in the reduction of the installed power itself, as this reduces the propeller thrust loading. Altogether this directs the way for a reduction of the propeller blade number, which in turns leads to a higher optimal rpm of the propeller and thereby LRM. Alternatively, a CP propeller will in theory be capable of attaining 100% engine speed and thereby 100% power in all conditions, offering the advantage that a pitch reduction is only performed when needed. However, in such evaluations, the reduced propeller efficiency of a CP propeller at the reduced pitch, required to attain 100% engine speed under the added resistance of adverse conditions, must not be forgotten.

5.1. Future work

Simple predictions of added wave resistance are difficult, and the three presented methods show differences on both the quantitative and qualitative levels. For their realistic use with respect to MPP, the methods need therefore to be compared against full-scale data or at least be compared to model tank tests or numerical simulations in the next phase. Despite the lack of a consistent method to *measure* added wave resistance when a real-sized ship operates in a seaway, possible approaches have been suggested by [18] and [40].

The interaction between waves, a ship, and its propulsion plant is highly dynamic and *not* static as has been assumed in the present study, and also assumed by the MPP-guidelines [1]. As ship speeds are expected to decrease further, as future efficiency requirements are tightened to meet the emission targets of the IMO, it will be relevant to evaluate not only how a ship performs with respect to the mean added wave resistance, but also to evaluate how the ship and propulsion plant perform dynamically, addressing the wave-induced response by establishing a model of the engine, turbo charger, shafting, and propeller. Furthermore, such a dynamic evaluation should include a study about the effect of the sea state on variations on the wake and thrust deduction factors, e.g. [41, 42], along with consideration of the effects of dynamic propeller ventilation. In addition,

the propulsion plant's capability to accelerate itself and respond to the actual added resistance in a dynamic seaway must be evaluated, not only with respect to the static load limits of the main engine but also with respect to the dynamic load limits. Such evaluations are outstanding and are recommended to be performed, at least in order to verify that the static consideration, on which the present IMO guidelines is based, can be justified as a basis for future power reductions.

Acknowledgment

The idea to adjust the pitch radius of gyration in STA-wave2 was formulated during discussions between MAN Energy Solutions and Jan Wienke, DNV GL, and the contribution is appreciated. The work by the second author has been supported by the Research Council of Norway through the Centres of Excellence funding scheme, project number 223254 AMOS.

References

[1] Marine Environment Protection Committee, 2013 Interim Guidelines for determining minimum propulsion power to maintain the manoeuvrability of ships in adverse conditions, IMO Circular MEPC 71/Circ.850/Rev.2, International Maritime Organization, London, UK (2017).

[2] Marine Environment Protection Committee, 2018 Guidelines on the Method of Calculation of the Attained Energy Efficiency Design Index (EEDI) for New Ships, IMO Circular MEPC.308(73), International Maritime Organization, London, UK (2018).

[3] ITTC, Recommended procedures and guidelines. Seakeeping Experiments, Tech. rep., 28th International Towing Tank Conference, Wuxi, China (2017).

[4] ITTC, Recommended procedures and guidelines. Prediction of Power Increase in Irregular Waves from Model Test, Tech. rep., 27th International Towing Tank Conference, Copenhagen, Denmark (2014).

[5] Marine Environment Protection Committee, Draft revised guidelines for determining minimum propulsion power to maintain the manoeuvrability of ships in adverse conditions, IMO Circular MEPC 71/INF.28, International Maritime Organization, London, UK (2017).

[6] Marine Environment Protection Committee, Supplementary information on the draft revised guidelines for determining minimum propulsion power to maintain the manoeuvrability of ships in adverse conditions, IMO Circular MEPC 71/INF.29, International Maritime Organization, London, UK (2017).

[7] S. Liu, B. Shang, A. Papanikolaou, On the resistance and speed loss of full type ships in a seaway, Ship Technology Research 66 (2019) 161–179.

[8] J. Ström-Tejsen, H. Yeh, D. Moran, Added resistance in waves, Trans. SNAME 81 (1973) 109–143.

[9] O. Faltinsen, Sea Loads on Ships and Offshore Structures, Cambridge University Press, 1990.

[10] J. N. Newman, Marine Hydrodynamics, MIT Press, 1977.

[11] S. Liu, A. Papanikolaou, Fast approach to the estimation of the added resistance of ships in head waves, Ocean Engineering 112 (2016) 211–225.

[12] S. Liu, A. Papanikolaou, Regression analysis of experimental data for added resistance in waves of arbitrary heading and development of a semi-empirical formula, Ocean Engineering 206 (2020) 107357.

[13] H. van den Boom, I. van der Hout, M. Flikkema, Speed-Power Performance of Ships during Trials and in Service, Sta-jip report, MARIN, The Netherlands (2008).

[14] ITTC, Analysis of speed/power trial data. Recommended Procedures and Guidelines, Tech. rep., 27th International Towing Tank Conference, Copenhagen, Denmark (2014).

[15] British Standard, ISO 15016: Ships and marine technology - Guidelines for the assessment of speed and power performance by analysis of speed trial data, BSI Standards Limited, 2015.

[16] K. Rawson, E. Tupper, Basic Ship Theory, 5th ed., Elsevier, 2001.

[17] S. Liu, A. Papanikolaou, Approximation of the added resistance of ships with small draft or in Ballast condition by empirical formula, Proc. IME M J Eng Marit Environ. 231 (2017) 1–14.

[18] P. Holt, Design tool for preliminary evaluation of compliance with minimum propulsion power requirements, Master's thesis, Technical University of Denmark, Kgs. Lyngby, Denmark (July 2019).

[19] H. Söding, A. von Graefe, O. el Moctar, V. Shigunov, Rankine Source Method for Seakeeping Predictionsl, in: Proc. of 31st OMAE, Rio de Janeiro, Brazil, 2012.

[20] T. Gourlay, V. Shigunov, A. von Graefe, E. Lataire, Comparison Of Aqwa, GL Rankine, Moses, Octopus, Pdstrip And Wamit With Model Test Results For Cargo Ship Wave-Induced Motions In Shallow Water, in: Proc. of 34th OMAE, St. John's, Newfoundland, Canada, 2015.

[21] V. Bertram, Added Power in Waves Time to Stop Lying (to Ourselves), in: Proceedings of 1st HullPIC Confence, Castello di Pavone, Italy, 2016, pp. 5–13.

[22] E. Buckingham, On physically similar systems, illustrations of the use of dimensional equations, Physical Review 4 (1914) 345–376.

[23] C. Nielsen, A ship design tool for estimating added resistance in waves, Master's thesis, Technical University of Denmark, Kgs. Lyngby, Denmark (2015).

[24] M. Martinsen, A design tool for estimating wave added resistance of container ships, Master's thesis, Technical University of Denmark, Kgs. Lyngby, Denmark (2016).

[25] N. Salvesen, Added resistance in waves, Journal of Hydronautics 12 (1978) 24–34.

[26] O. Faltinsen, K. Minsaas, N. Liapis, S. Skjørdal, Prediction of resistance and propulsion of a ship in a seaway, in: Proc. 13th Symposium on Naval Hydrodynamics, Tokyo, Japan, 1980.

[27] ITTC, 1978 ITTC Performance Prediction Method, Tech. rep., International Towing Tank Conference, Rio de Janeiro, Brazil (2011).

[28] H. Guldhammer, S. Harvald, Ship Resistance (revised edition), Akademisk Forlag, 1974.

[29] J. Holtrop, G. Mennen, An approximate power prediction method, J. Intl. Shipbuilding Progress 29 (1982) 166–170.

[30] H.O.H. Kristensen and H.B. Bingham, Prediction of Resistance and Propulsion Power of Ships, Project no. 2016-108 no. 04, Technical University of Denmark, Kgs. Lyngby, Denmark (2017).

[31] H.O.H. Kristensen and H.B. Bingham, Manual for the SHIP-DESMO computer program for exhaust gas emission calculations for container ships, Project no. 2016-108 no. 06, Technical University of Denmark, Kgs. Lyngby, Denmark (2017).

[32] T. F. M. Ueno, Y. Ikeda, A new estimation method of wind forces and moments acting on ships on the basis of physical component methods (in Japanese), J. Japan S. of Naval Arch. and Ocean Engineers 2 (2005) 243–255.

[33] T. Fujiwara, Y. Tsukada, F. Kitamura, H. Sawada, S. Ohmatsu, Experimental investigation and estimation on wind forces for a container ship, in: Proc. 19th ISOPE, Osaka, Japan, 2009.

[34] MAN Energy Solutions, Basic Principles of Ship Propulsion, MAN, 2018, available online: www.man-es.com.

[35] W. van Lammeren, J. van Manen, M. Oosterveld, The Wageningen B-screw Series, SNAME Trans. 77 (1969) 269–317.

[36] S. Harvald, Resistance and Propulsion of Ships, John Wiley, 1983.

[37] R. Grin, On the Prediction of Wave-added Resistance with Empirical Methods, J. Ship Production and Design 31 (2015) 181–191.

[38] MAN B&W Dielsel A/S, Instruction Manual: Operation 704-03 Edition 0001, Tech. rep. (20xx).

[39] Y. Goda, Random Seas and Design of Maritime Structures, Vol. 15 of Advanced Series on Ocean Engineering, World Scientific, 2000.

[40] U. D. Nielsen, J. Johannesen, H. Bingham, M. Blanke, S. Joncquez, Indirect Measurements of Added-wave Resistance On an In-service Container Ship, in: T. Okada, K. Suzuki, Y. Kawamura (Eds.), PRADS 2019, Springer Nature, Yokohama, Japan, 2019, pp. 115–132.

[41] B. Taskar, K. Yum, S. Steen, E. Pedersen, The effect of waves on engine-propeller dynamics and propulsion performance of ships, Ocean Engineering 122 (2016) 262–277.

[42] B. Taskar, P. Regener, P. Andersen, The impact of propulsion factors on vessel performance in waves, in: Proc. of 6th Int'l Symp. on Marine Propulsors, Rome, Italy, 2019.